Electronic Supplementary Material (ESI) for Journal of Materials Chemistry A

Supporting Information

Self-assembly of individual polymer chain-metal nanoparticles for polymer cargo nanocomposites with tunable properties

Md. Shahinul. Islam[a], *Won San Choi*[b]*, *Young Boo Lee*[a], *and Ha-Jin Lee*[a]*

Detailed Experimental Methods

Synthesis of the Alloy-type Multi-metallic NP-PECs by the Coreduction Method: For the synthesis of the alloy-type and core-shell-type multi-metallic NP-PECs, PAH-Au^{-}, PAH-Pt^{-}, PAA-Ag^{+} and PAA-Pd^{+} were prepared for the multi-metallic NP-PECs containing individual metal NPs; these ionic species were used in equivalent concentrations and quantities.

The mixed solution of PAA-Ag^{+} and PAA-Pd^{+} was added dropwise into the mixed solution of PAH-Au^{+} and PAH-Pt^{+}, each in equal volume ratios (1:1:1:1). The alloy-type tetra-metallic NP-PECs were prepared by further stirring for 1 h followed by heat treatment at 150 °C in a furnace for 1 h. The tri-metallic NP-PECs were obtained by thermal reduction of the mixture solution, which was prepared by the dropwise addition of a mixed solution of PAA-Ag^{+} solution and PAA-Pd^{+} (25% each) into a PAH-Au^{-} solution (50%) followed by thermal reduction. The bi-metallic NP-PECs were obtained from the dropwise addition of PAA-Ag^{+} into PAH-Au^{+} in an equal volume ratio (1:1) followed by thermal reduction.

Synthesis of the Core-Shell-type Multi-metallic NP-PECs by the Successive Reduction Procedure: 1 mL of aqueous PAH-Pt^{+} solution was slowly added into 1 mL of aqueous PAH-AuNPs while stirring, and the mixture was thermally treated at 150 °C for 1 h. The resulting material was denoted as PAH-Au/Pt. Next, 1 mL of aqueous PAA-Ag^{+} solution was slowly added into the aqueous PAH-Au/Pt solution while stirring, and the mixture was thermally treated at 150 °C for 1 h. The resulting material was denoted as PEC-Au/Pt/Ag. Finally, 1 mL of aqueous PAA-Pd^{+} solution was slowly added into the aqueous PEC-Au/Pt/Ag solution, and the mixture was treated at 150 °C for 1 h. It is important that the total mixture volume ratio of metal NP-embedded PAH and PAA should be equal (1:1).

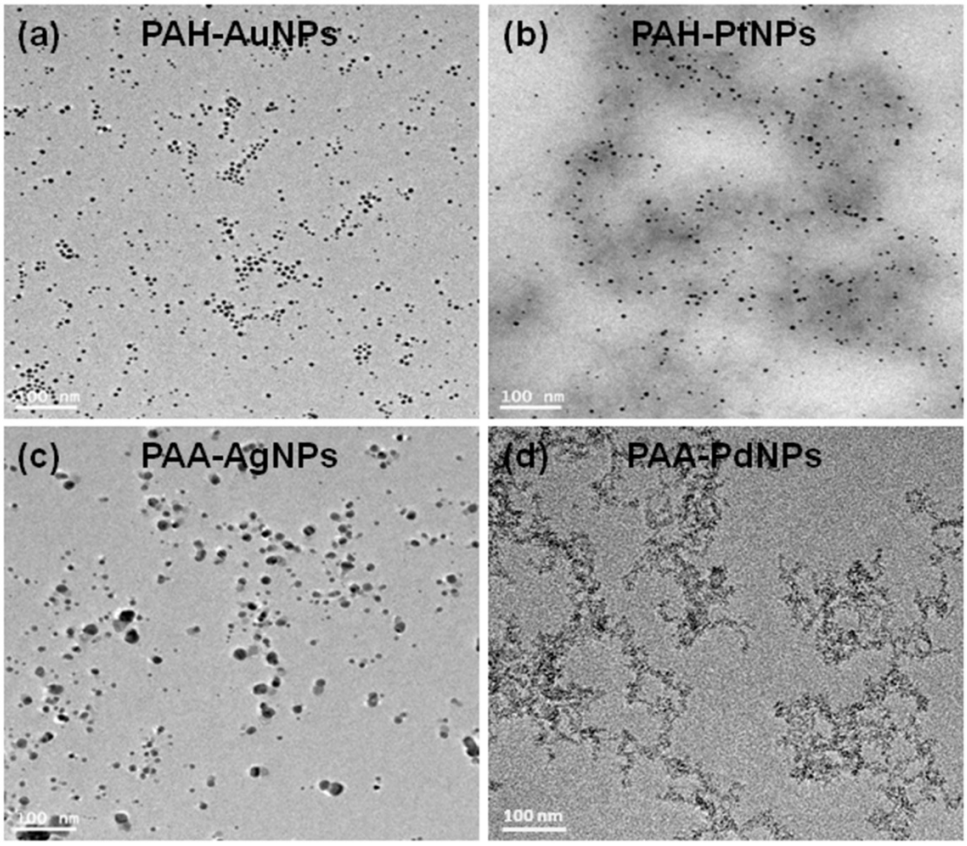

Fig. S1 TEM images of the (a) PAH-AuNPs, (b) PAH-PtNPs, (c) PAA-AgNPs and (d) PAA-PdNPs.

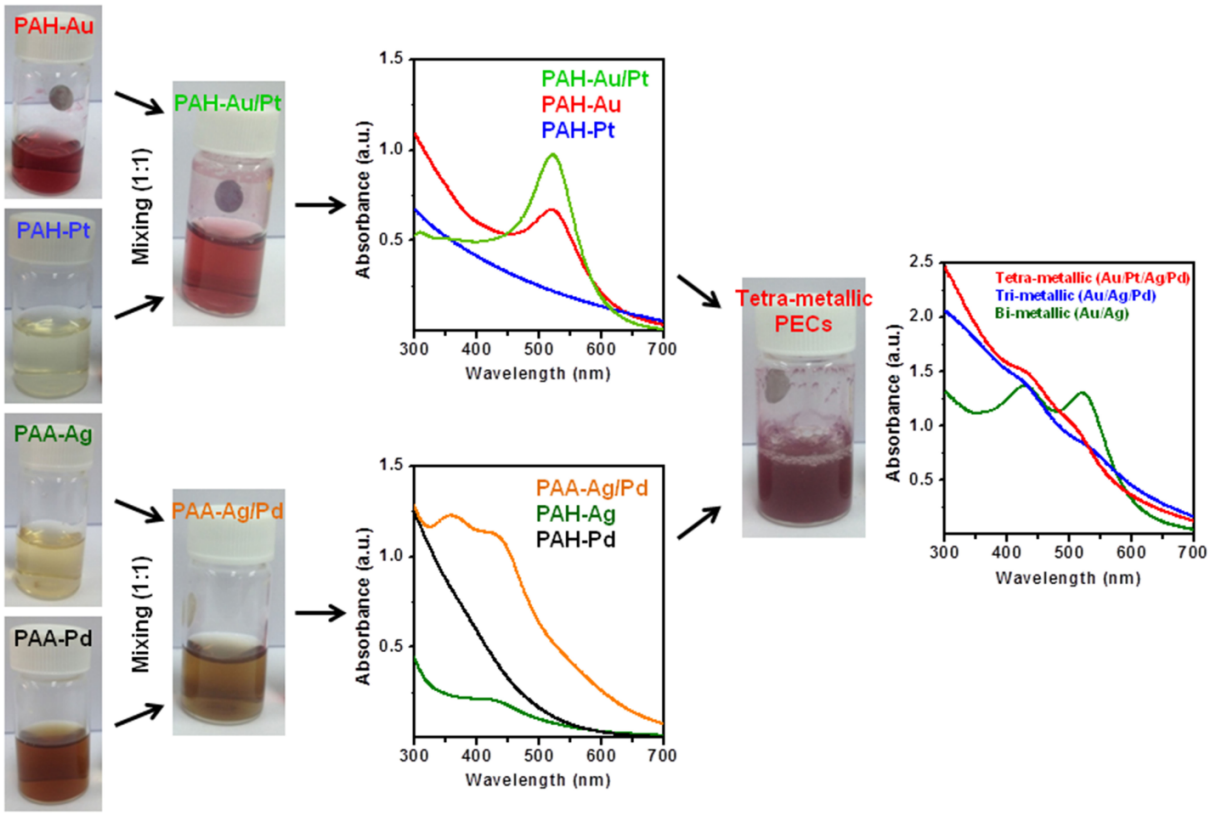

Fig. S2 Solution images of the PE-metal NPs and the multi-metallic NP-PECs, and the corresponding UV-vis absorbance data.

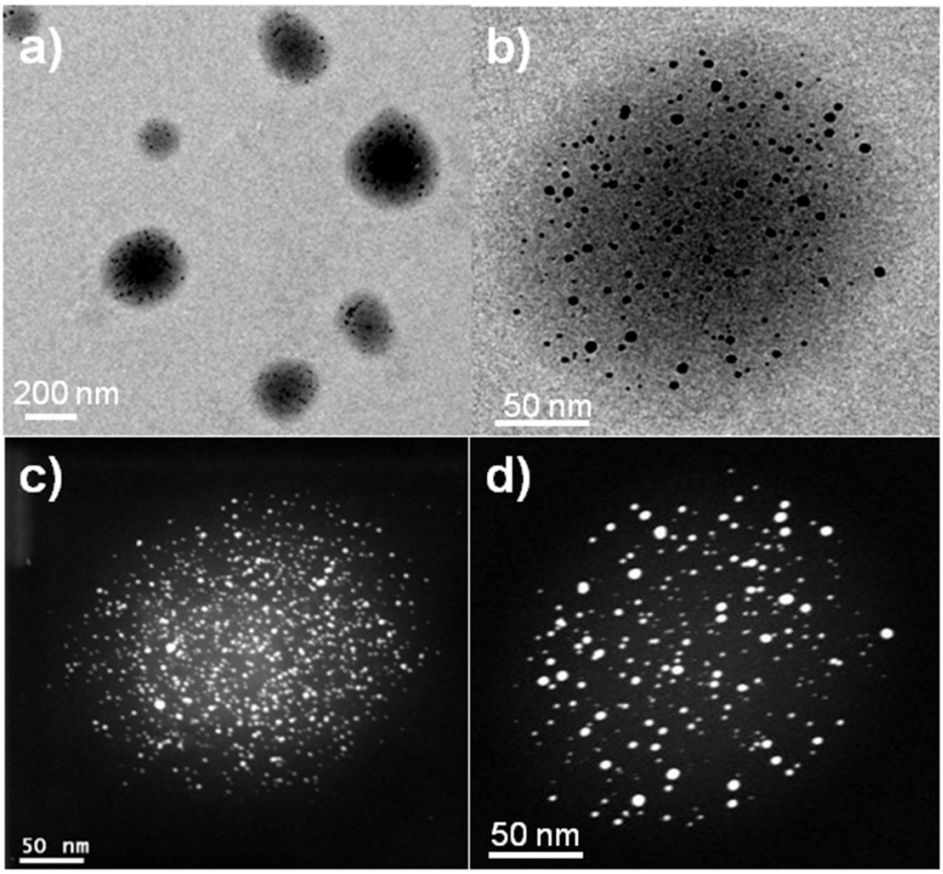

Fig. S3 (a, b) TEM and (c, d) STEM images of the bi-metallic NP-PECs, PEC-Au_{50}/Ag_{50}.

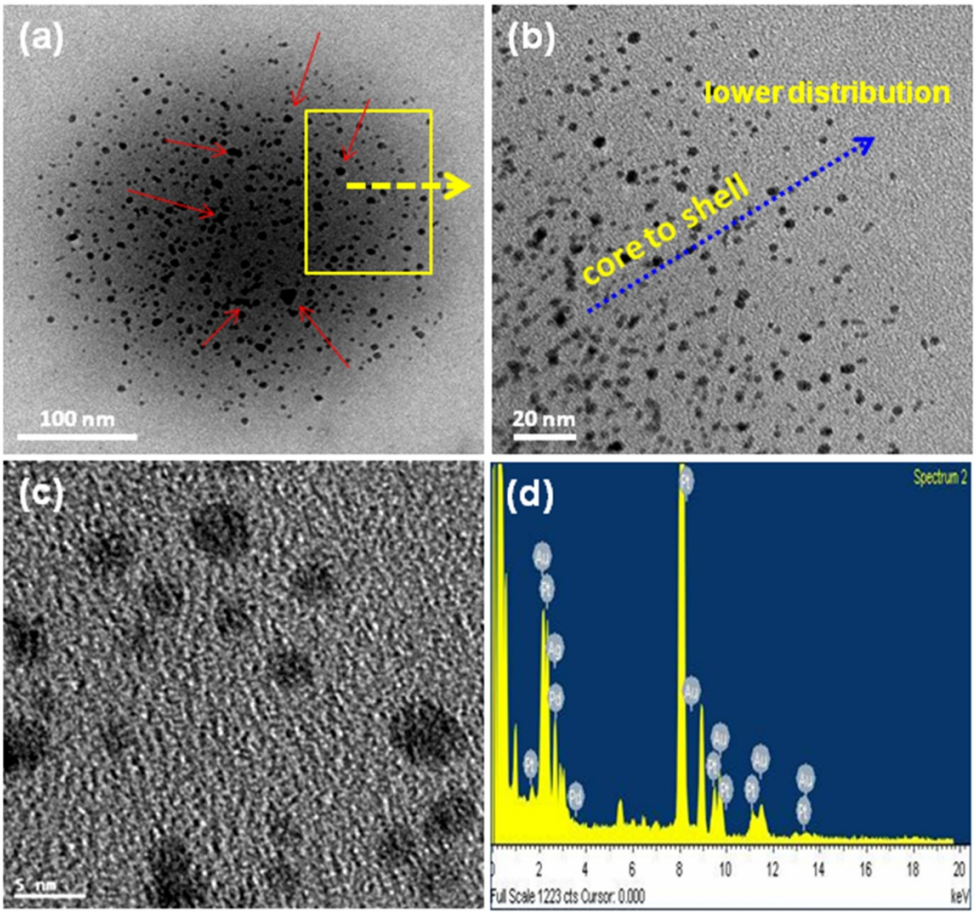

Fig. S4 (a-c) TEM and (d, e) STEM images of PEC-$Au_{25}/Pt_{25}/Ag_{25}/Pd_{25}$ showing the distribution of metal NPs within the PECs. (f) The EDS data ensure the existence of four types of metal NPs within the PECs.

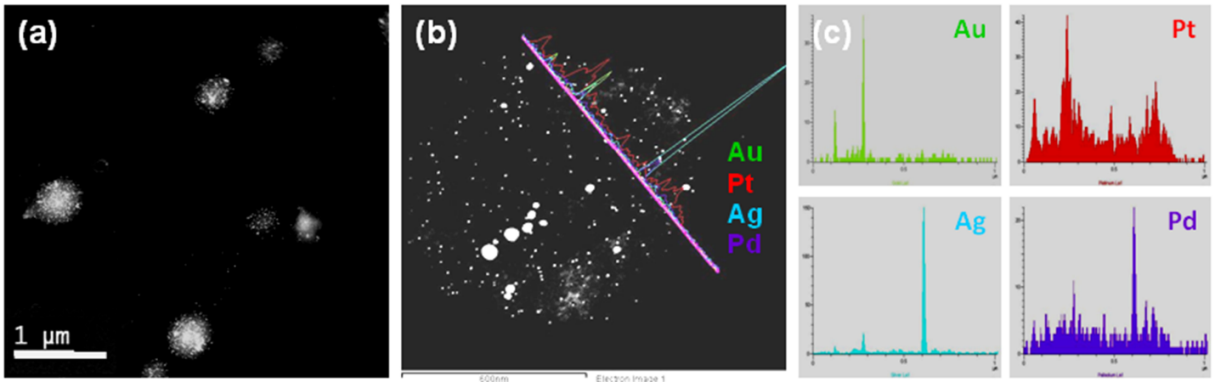

Fig. S5 (a, b) STEM images and (c) the line-scan EDS data of PEC-$Au_{15}/Pt_{35}/Ag_{25}/Pd_{25}$.

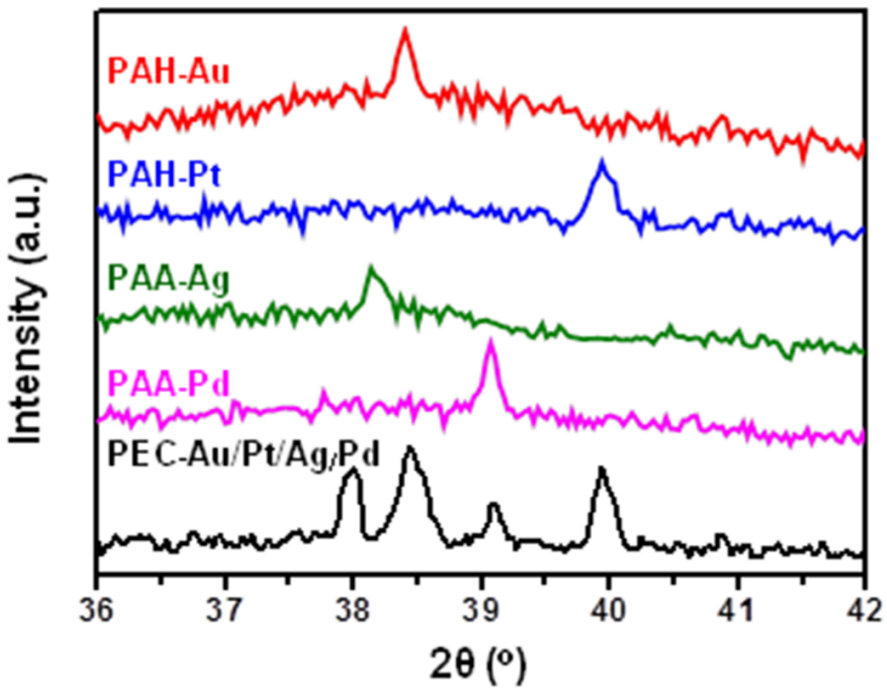

Fig. S6 XRD patterns of the four types PE-metal NPs and PEC-$Au_{25}/Pt_{25}/Ag_{25/}Pd_{25}$.

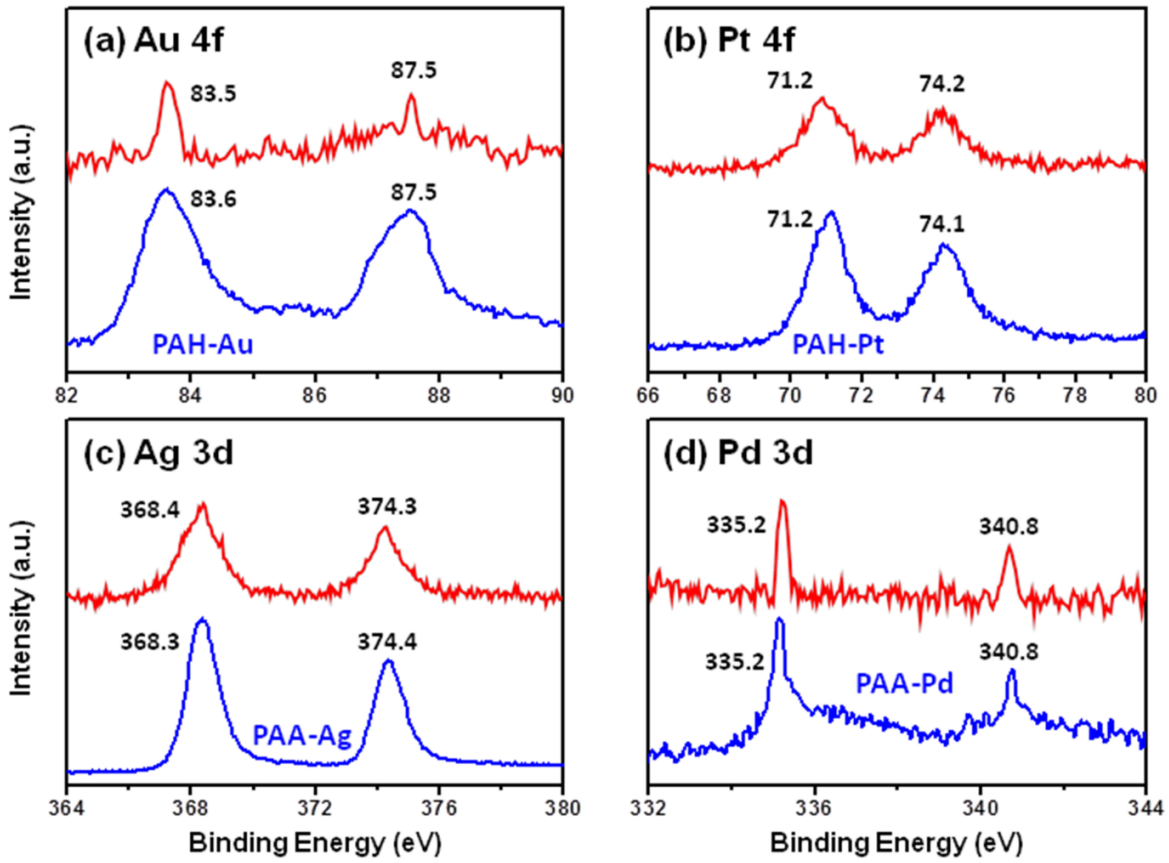

Fig. S7 XPS spectra of the PE-metal NPs (the blue lines) and PEC-$Au_{25}/Pt_{25}/Ag_{25}/Pd_{25}$ (the red lines).

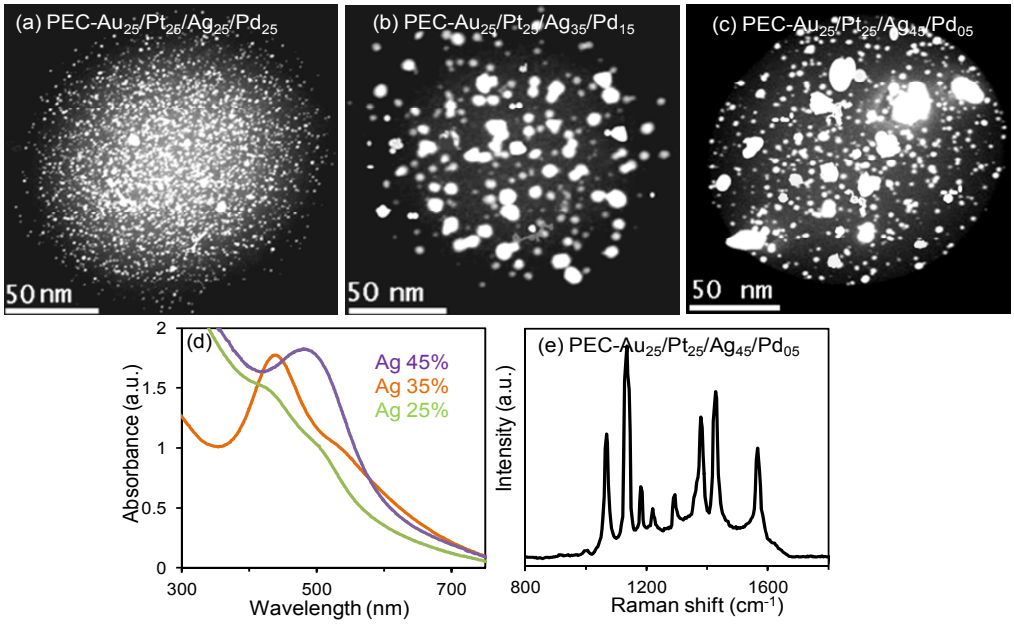

Fig. S8 (a-c) STEM images for tetra-metallic NP-PECs with various ratios of AgNPs prepared by proposed individual mixing method. (d) UV-vis absorption data exhibiting red shift of absorbance with increasing fraction of Ag from 25 to 40%. Curve (Green) PEC-$Au_{25}/Pt_{25}/Ag_{25}/Pd_{25}$, (Orange) PEC-$Au_{25}/Pt_{25}/Ag_{35}/Pd_{15}$, and (Violet) PEC-$Au_{25}/Pt_{25}/Ag_{45}/Pd_{05}$. (e) Raman spectrum obtained by PEC-$Au_{25}/Pt_{25}/Ag_{45}/Pd_{05}$ onto 4-ATP surface.

Sample	Zeta potential (mV)
PAH	+64.54
PAH-AuNPs	+30.23
PAH-PtNPz	+33.92
PAA	-49.83
PAA-AgNPs	-20.57
PAA-PdNPs	-15.84
PECs	+40.67
PEC-Au_{50}/Ag_{50}	+16.10
PEC-$Au_{25}/Ag_{25}/Pd_{25}/Pt_{25}$	+5.29

Fig. S9 Zeta potential data of the PEs before and after attaching the four types of metal NPs, the bare PECs and PEC-$Au_{25}/Pt_{25}/Ag_{25}/Pd_{25}$.

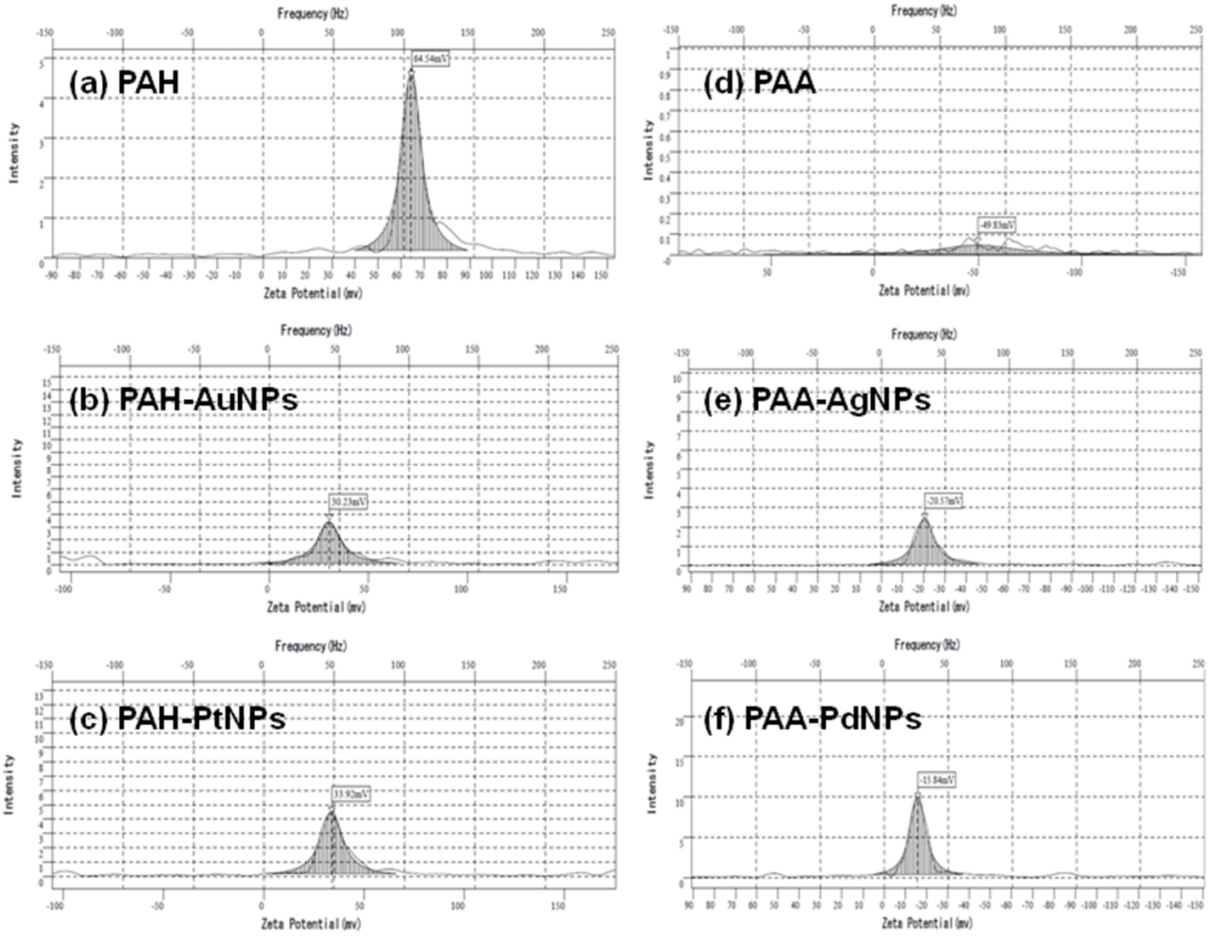

Fig. S10 Zeta potential data of the PEs before and after attaching the four types of metal NPs.

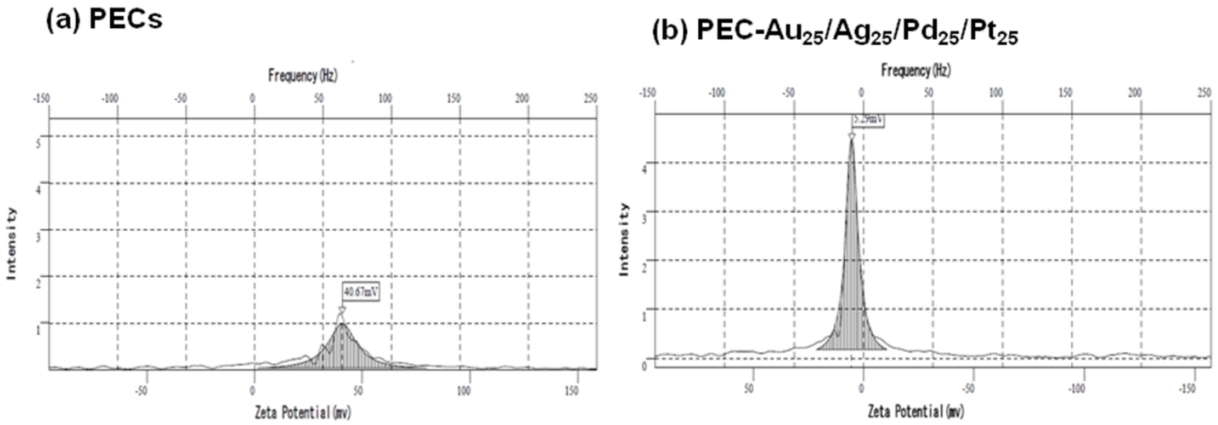

Fig. S11 Zeta potential data of the bare PECs and PEC-$Au_{25}/Pt_{25}/Ag_{25/}Pd_{25}$.

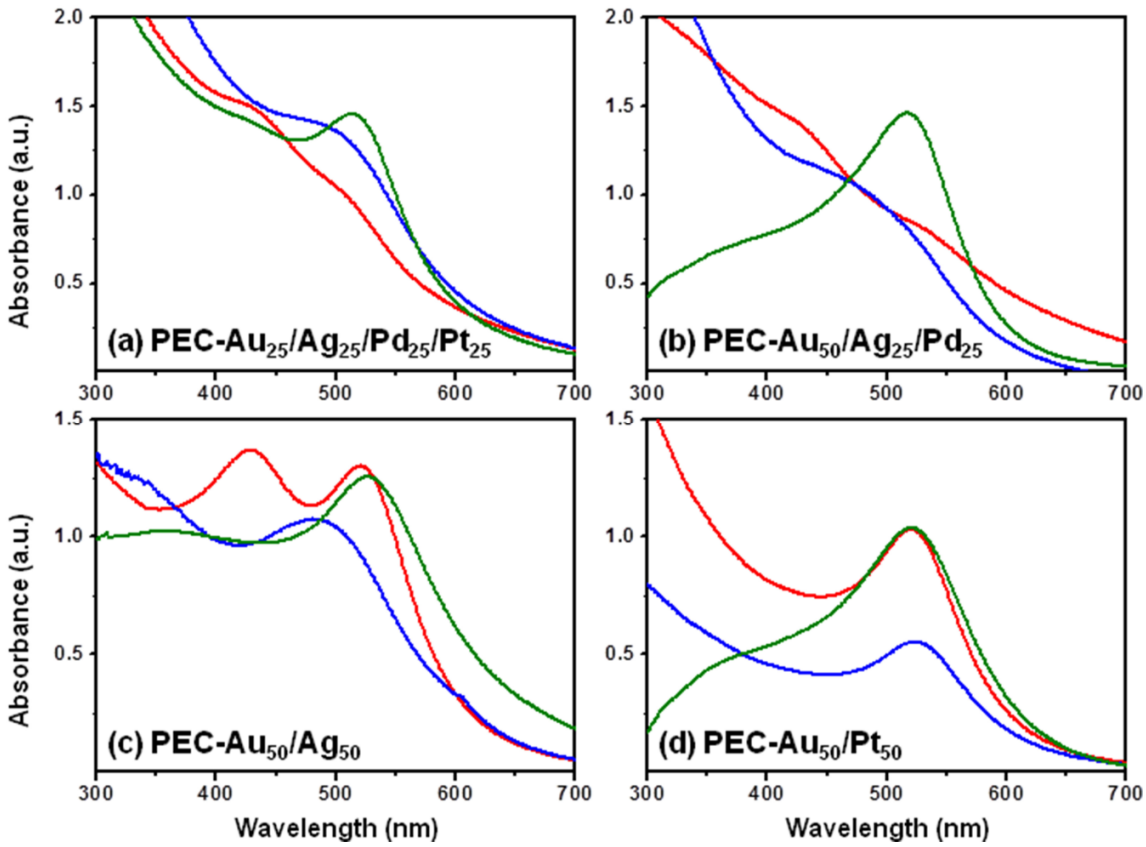

Fig. S12 UV-vis absorption data of the multi-metallic NP-PECs. The multi-metallic NP-PECs were prepared by three different methods, including our method (the red lines), the coreduction method (the blue lines) and the successive reduction method (the green lines).

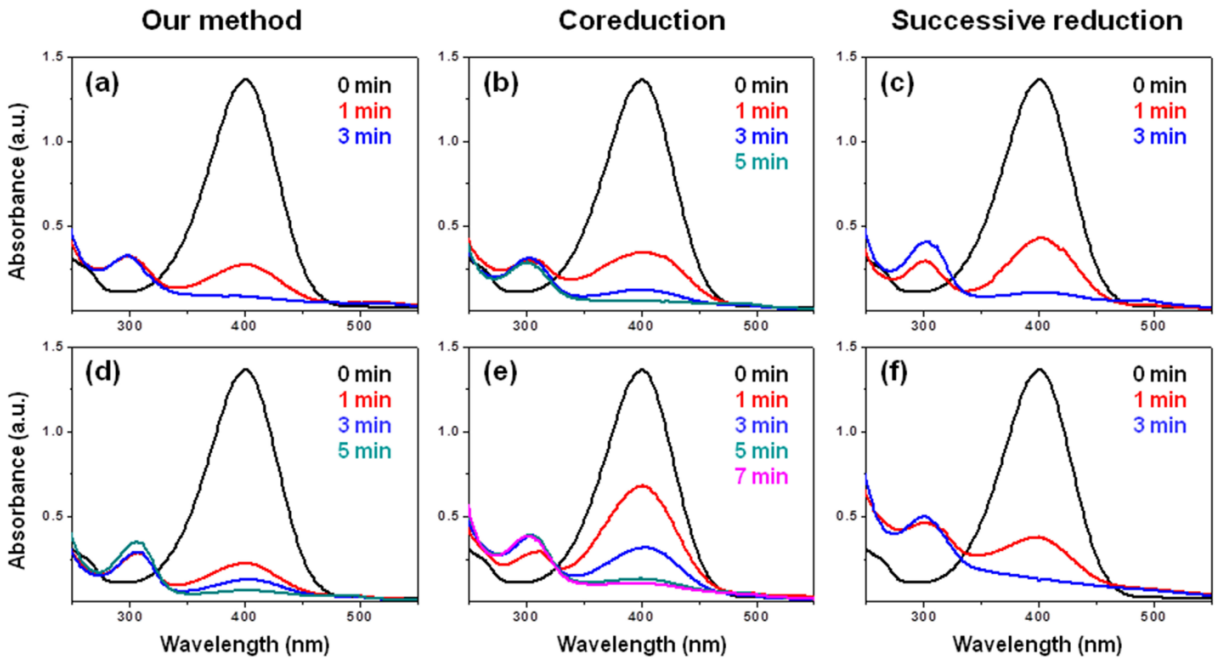

Fig. S13 Time-dependent UV-vis absorption spectral changes for the reduction of 4-NPh in the presence of (a-c) the tetra-metallic NP-PECs and (d-f) the tri-metallic NP-PECs. Both multi-metallic NP-PECs were prepared by each of the three different methods.

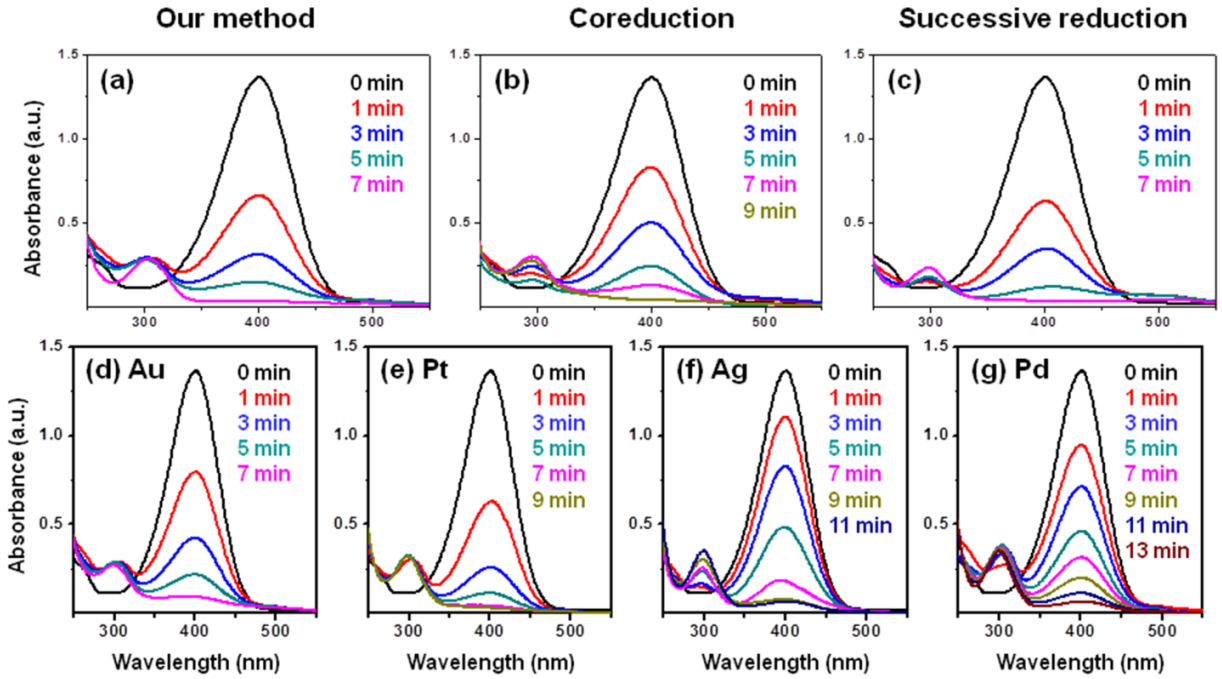

Fig. S14 Time-dependent UV-vis absorption spectral changes for the reduction of 4-NPh in the presence of (a-c) the bi-metallic NP-PECs and (d-g) the PE-metal NPs. The bi-metallic NP-PECs were prepared by the three different methods.

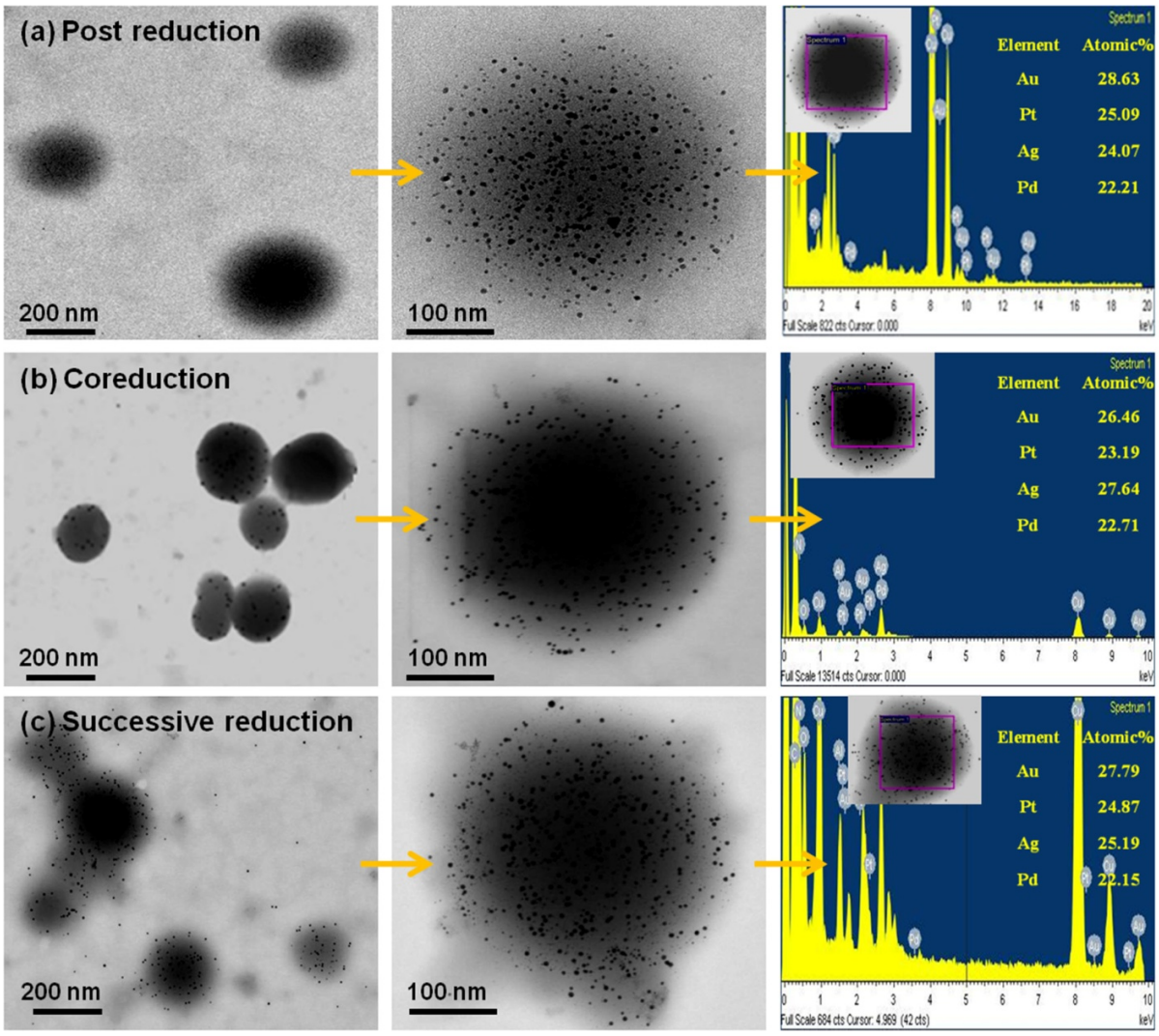

Fig. S15 TEM images and the relevant EDS data of the tetra-metallic NP-PECs prepared by (a) our method, (b) the coreduction method and (c) the successive reduction method. The four types of metal precursors were used with equal volume ratios for all three methods. All multi-metallic cases prepared by the three different methods show approximately similar individual metal compositions in the multi-components.

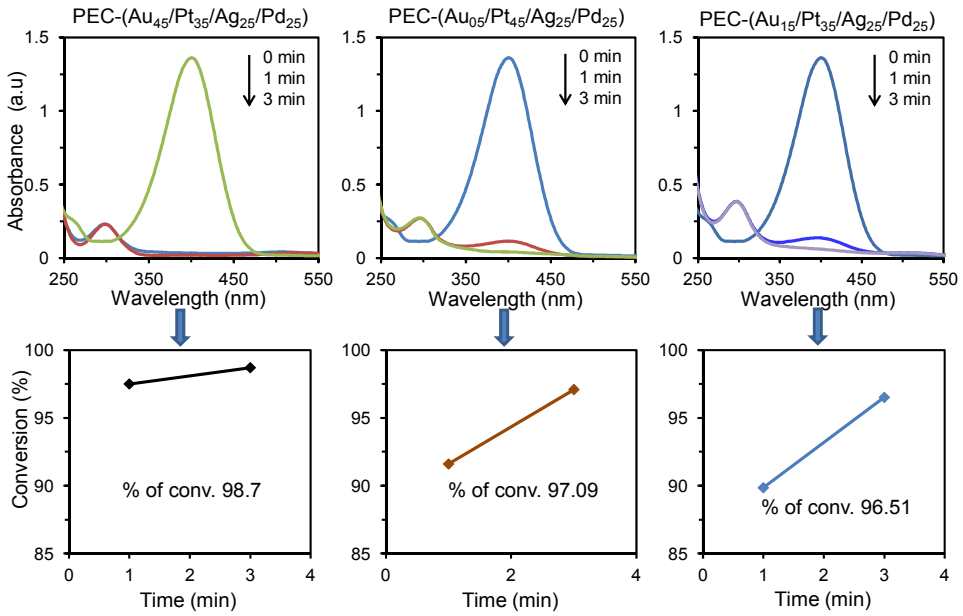

Fig. S16 Comparative UV-vis absorbance spectra and their corresponding % of conversion for catalytic reduction of 4-NPh to 4-APh using the PEC-Au/Pt/Ag/Pd as a function of Au content.

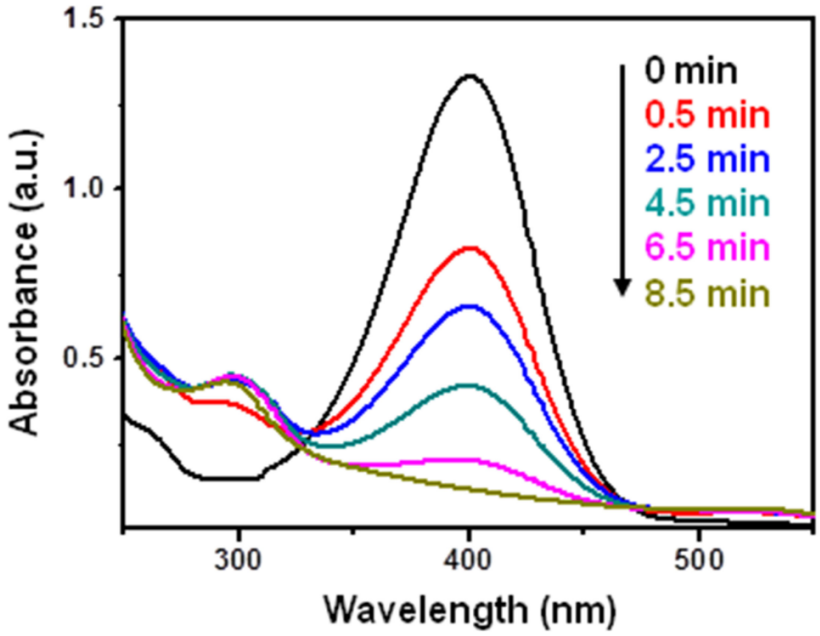

Fig. S17 Time-dependent UV-vis absorption spectral changes for the reduction of 4-NPh in the presence of PEC-AuNPs.